CMB power spectrum estimation with non-circular beam and incomplete sky coverage

Sanjit Mitra,[1,*] Anand S. Sengupta,[2,†] Subharthi Ray,[1,‡] Rajib Saha,[3,1,§] and Tarun Souradeep[1,¶]

[1] *Inter-University Centre for Astronomy and Astrophysics, Post Bag 4, Ganeshkhind, Pune 411007, India.*
[2] *School of Physics and Astronomy, Cardiff University, 5, The Parade, Cardiff CF24 3YB, U.K.*
[3] *Indian Institute of Technology, Kanpur, Kanpur 208 016, India*

Over the last decade, measurements of the CMB anisotropy has spearheaded the remarkable transition of cosmology into a precision science. However, addressing the systematic effects in the increasingly sensitive, high resolution, 'full' sky measurements from different CMB experiments pose a stiff challenge. The analysis techniques must not only be computationally fast to contend with the huge size of the data, but, the higher sensitivity also limits the simplifying assumptions which can then be invoked to achieve the desired speed without compromising the final precision goals. While maximum likelihood is desirable, the enormous computational cost makes the suboptimal method of power spectrum estimation using Pseudo-C_l unavoidable for high resolution data. The debiasing of the Pseudo-C_l needs account for non-circular beams, together with non-uniform sky coverage. We provide an analytic framework for correcting the power spectrum for the effect of beam non-circularity and non-uniform sky coverage (including incomplete/masked sky maps). The approach is perturbative in the distortion of the beam from non-circularity allowing for rapid computations when the beam is mildly non-circular. When non-circular beam effect is important, we advocate that it is computationally advantageous to employ 'soft' azimuthally apodized masks whose spherical harmonic transform die down fast with m.

PACS numbers: 98.70.Vc,95.75.Pq,98.80Es

I. INTRODUCTION

The fluctuations in the Cosmic Microwave Background (CMB) radiation are theoretically very well understood, allowing precise and unambiguous predictions for a given cosmological model [1, 2]. The measurement of these CMB anisotropy with the ongoing Wilkinson Microwave Anisotropy Probe (WMAP) and the upcoming Planck surveyor, has ushered in a new era of precision cosmology. Such data rich experiments, with increased sensitivity, high resolution and 'full' sky measurements pose a stiff challenge for current analysis techniques to realize the full potential of precise determination of cosmological parameters. The analysis techniques must not only be computationally fast to contend with the huge size of the data, but, the higher sensitivity also limits the simplifying assumptions that can then in invoked to achieve the desired speed without compromising the final accuracy. As experiments improve in sensitivity, the inadequacy in modeling the observational reality start to limit the returns from these experiments. The current effort is to push the boundary of this inherent compromise faced by the current CMB experiments that measure the anisotropy in the CMB temperature and polarization.

Accurate estimation of the angular power spectrum, C_l, is inarguably the foremost concern of most CMB experiments. The extensive literature on this topic has been summarized [1, 2, 3]. For Gaussian, statistically isotropic CMB sky, the C_l that corresponds to the covariance that maximizes the multivariate Gaussian PDF of the temperature map, $\Delta T(\hat{\mathbf{q}})$, is the Maximum Likelihood (ML) solution. Different ML estimators have been proposed and implemented on CMB data of small and modest sizes [4, 5, 6, 7, 8, 9]. While it is desirable to use optimal estimators of C_l that obtain (or iterate toward) the ML solution for the given data, these methods are usually limited by the computational expense of matrix inversion that scales as N_d^3 with data size N_d [10, 11]. Various strategies for speeding up ML estimation have been proposed, such as, exploiting the symmetries of the scan strategy [12], using hierarchical decomposition [13], iterative multi-grid method [14], etc. Variants employing linear combinations of $\Delta T(\hat{\mathbf{q}})$ such as

*Electronic address: sanjit@iucaa.ernet.in; (Present address: Département ARTEMIS Observatoire de la Côte d'Azur, BP 4229 06304 Nice Cedex 4 France; e-mail:sanjit@oca.eu)
†Electronic address: Anand.Sengupta@astro.cf.ac.uk
‡Electronic address: sray@iucaa.ernet.in
§Electronic address: rajib@iitk.ac.in
¶Electronic address: tarun@iucaa.ernet.in

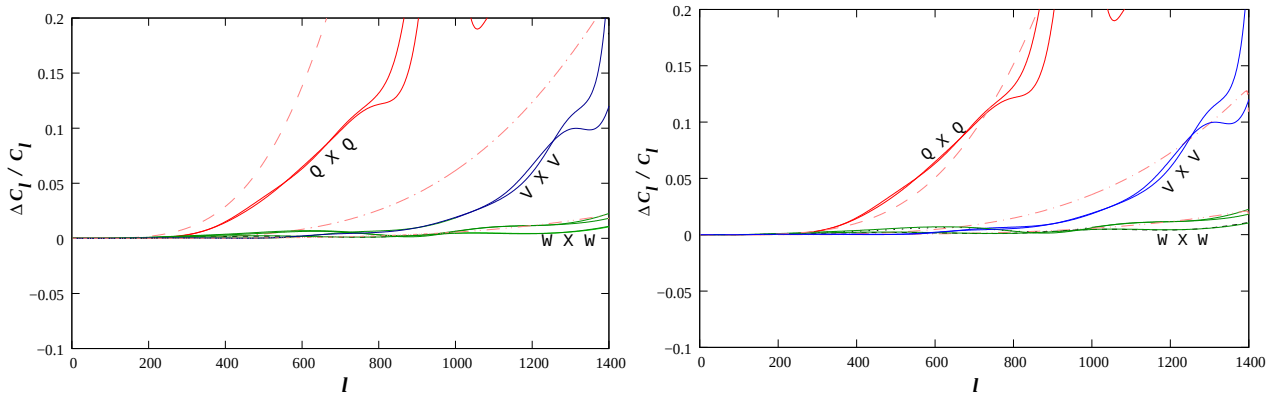

FIG. 1: The predicted non-circular beam correction for a CMB experiment with elliptical Gaussian beam with *fwhm* beam-width of 0.51° and eccentricity, $e = 0.65$ for the Q beam (dashed line), beam-width of 0.35° and $e = 0.46$ for the V beam (dash-dotted line) and beam-width of 0.22° and $e = 0.4$ for the W beam (dash-dot-dot line) are shown in the left plot. The solid curves are the non circular beam corrections estimated by the WMAP team for the Q,V and W channels. In the plot in the right, we show that the non-circular beam correction matches with the estimates of the WMAP team for a slightly different change in the eccentricity of the Q and V beams (W beams matched in the left plot), with the new eccentricities $e = 0.50$ and $e = 0.40$ respectively. This difference is attributed to the fact that the beams visit the pixels multiple times with different orientations, and hence the *effective* eccentricity is reduced.

a_{lm} on set of rings in the sky can alleviate the computational demands in special cases [15, 16]. Other promising 'exact' power estimation methods have been recently proposed [17, 18, 19].

However there also exist computationally rapid, sub-optimal estimators of C_l. Exploiting the fast spherical harmonic transform ($\sim N_d^{3/2}$), it is possible to estimate the angular power spectrum $C_l = \sum_m |a_{lm}|^2/(2l+1)$ rapidly [20, 21]. This is commonly referred to as the Pseudo-C_l method [22]. Analogous approach employing fast estimation of the correlation function $C(\hat{\mathbf{q}} \cdot \hat{\mathbf{q}}') \equiv \langle \Delta T(q) \Delta T(q') \rangle$ have also been explored [23, 24]. It has been recently argued that the need for optimal estimators may have been over-emphasized since they are computationally prohibitive at large l. Sub-optimal estimators are computationally tractable and tend to be nearly optimal in the relevant high l regime. Moreover, already the data size of the current sensitive, high resolution, 'full sky' CMB experiments, such as WMAP have been compelled to use sub-optimal Pseudo-C_l and related methods [25, 26]. On the other hand, optimal ML estimators can readily incorporate and account for various systematic effects, such as noise correlations, non-uniform sky coverage and beam asymmetries. A hybrid approach of using ML estimation of C_l for low l for low resolution map and Pseudo-C_l like estimation for large l where it is nearly optimal has been suggested [3] and has even been employed by the recent analysis of the WMAP-3 year data [32]. The systematic correction to the Pseudo-C_l power spectrum estimate arising from non-uniform sky coverage has been studied and implemented for CMB temperature [27] and polarization [28]. The systematic correction for non circular beam has been studied by us in an earlier publication [29]. Here we extend the results to include non-uniform sky coverage.

It has been usual in CMB data analysis to assume the experimental beam response to be circularly symmetric around the pointing direction. However, real beam response functions have deviations from circular symmetry. Even the main lobe of the beam response of experiments are generically non-circular (non-axisymmetric) since detectors have to be placed off-axis on the focal plane. (Side lobes and stray light contamination add to the breakdown of this assumption). For highly sensitive experiments, the systematic errors arising from the beam non-circularity become progressively more important. Dropping the circular beam assumption leads to major complications at every stage of the analysis pipeline. The extent to which the non-circularity of the beam affects the step of going from the time-stream data to sky map is very sensitive to the scan-strategy. The beam now has an orientation with respect to the scan path that can potentially vary along the path. This implies that the beam function is inherently time dependent and difficult to deconvolve.

Even after a sky map is made, the non-circularity of the effective beam affects the estimation of the angular power spectrum, C_l, by coupling the power at different multipoles, typically, on scales beyond the inverse angular beam-width. Mild deviations from circularity can be addressed by a perturbation approach [30, 31] and the effect of non-circularity on the estimation of CMB power spectrum can be studied (semi) analytically [29]. Figure 1 shows the predicted level of non-circular beam correction in our formalism for elliptical beams with *fwhm* beam-width of 0.22° compared to the non-circular beam corrections computed in the recent data release by WMAP [32].

To avoid contamination of the primordial CMB signal by Galactic emission, the region around the Galactic plane is masked from maps. If the Galactic cut is small enough, then the coupling matrix will be invertible, and the two-point

correlation function can be determined on all angular scales from the data within the uncut sky [33]. Hivon et al. [27] present a technique (MASTER) for fast computation of the power spectrum taking accounting for the galactic cut, but restricted to circular beams. In our present work, we present analytical expressions for the bias matrix of the Pseudo-C_l estimator for the incomplete sky coverage, *using a non-circular beam*. In Section II we show a heuristic approach to the analytic form of the bias matrix taking into account the above mentioned effects. We have shown that our estimation matches with the existing results in diferrent limits in Section III. In Section IV we outline the numerical implementation of our approach, estimate the computational cost and suggest a possible algorithmic route to reducing the cost. The discussion and conclusion of this work is given in Section V.

II. FORMALISM

The CMB temperature anisotropy field $\Delta T(\hat{\mathbf{q}})$ over all the sky directions $\hat{\mathbf{q}} \equiv (\theta, \phi)$ is assumed to be Gaussian and statistically isotropic and hence the angular power spectrum stores all the statistical information about the anisotropy field. These temperature fluctuations are expanded in the basis of spherical harmonics,

$$\Delta T(\hat{\mathbf{q}}) \;=\; \sum_{lm} a_{lm}\, Y_{lm}(\hat{\mathbf{q}}), \tag{2.1}$$

where a_{lm} are the spherical harmonic transforms of the temperature anisotropy field

$$a_{lm} \;\equiv\; \int_{4\pi} d\Omega_{\hat{\mathbf{q}}}\, \Delta T(\hat{\mathbf{q}})\, Y^*_{lm}(\hat{\mathbf{q}}). \tag{2.2}$$

The observed CMB temperature fluctuation field $\widetilde{\Delta T}(\hat{\mathbf{q}})$ is the convolution of the "beam" profile $B(\hat{\mathbf{q}}, \hat{\mathbf{q}}')$ with the real temperature fluctuation field $\Delta T(\hat{\mathbf{q}}')$ and contaminated by additive experimental noise $n(\hat{\mathbf{q}})$. Moreover, due to the strong influence of the foreground emission in our galactic plane and point sources, some of the pixels have to be masked prior to power spectrum estimation. The mask function $U(\hat{\mathbf{q}})$ is usually assigned zero for the corrupt pixels and one for the clean ones, but it could be a smoother weight function also, that can take values between zero and one, as long as it sufficiently masks the foreground contamination. Mathematically the observed temperature can be expressed as

$$\widetilde{\Delta T}(\hat{\mathbf{q}}) \;=\; U(\hat{\mathbf{q}}) \left[\int_{4\pi} d\Omega_{\hat{\mathbf{q}}'}\, B(\hat{\mathbf{q}}, \hat{\mathbf{q}}')\, \Delta T(\hat{\mathbf{q}}') \;+\; n(\hat{\mathbf{q}}) \right]. \tag{2.3}$$

Statistical isotropy of CMB anisotropy implies that the two point correlation function $C(\hat{\mathbf{q}}_1, \hat{\mathbf{q}}_2) = \langle \Delta T(\hat{\mathbf{q}}_1) \Delta T(\hat{\mathbf{q}}_2) \rangle$ depends only on the angular separation of the direction, i.e., $C(\hat{\mathbf{q}}_1, \hat{\mathbf{q}}_2) = C(\hat{\mathbf{q}}_1 \cdot \hat{\mathbf{q}}_2)$. We can therefore expand it as a Fourier-Legendre series

$$\langle \Delta T(\hat{\mathbf{q}}_1) \Delta T(\hat{\mathbf{q}}_2) \rangle \;=\; \sum_{l=0}^{\infty} \frac{2l+1}{4\pi} C_l\, P_l(\hat{\mathbf{q}}_1 \cdot \hat{\mathbf{q}}_2), \tag{2.4}$$

where the coefficients C_l constitute the CMB power spectrum

$$C_l \;\equiv\; \int_{4\pi} d\Omega_{\hat{\mathbf{q}}_1} \int_{4\pi} d\Omega_{\hat{\mathbf{q}}_2} \langle \Delta T(\hat{\mathbf{q}}_1)\, \Delta T(\hat{\mathbf{q}}_2) \rangle\, P_l(\hat{\mathbf{q}}_1 \cdot \hat{\mathbf{q}}_2). \tag{2.5}$$

The addition theorem for spherical harmonics

$$\frac{4\pi}{2l+1} \sum_{m=-l}^{l} Y^*_{lm}(\hat{\mathbf{q}}_1)\, Y_{lm}(\hat{\mathbf{q}}_2) \;=\; P_l(\hat{\mathbf{q}}_1 \cdot \hat{\mathbf{q}}_2), \tag{2.6}$$

and the orthogonality of Legendre polynomials

$$\int_{-1}^{1} dx\, P_l(x)\, P_{l'}(x) \;=\; \frac{2}{2l+1}\, \delta_{ll'} \tag{2.7}$$

can then be used to show that the matrix $\langle a_{lm} a_{l'm'} \rangle$ is diagonal

$$\langle a_{lm} a_{l'm'} \rangle \;=\; C_l\, \delta_{ll'}\, \delta_{mm'}. \tag{2.8}$$

The observed two point correlation function for a statistically isotropic CMB anisotropy signal is

$$\widetilde{C}(\hat{\mathbf{q}},\hat{\mathbf{q}}') = \langle\widetilde{\Delta T}(\hat{\mathbf{q}})\widetilde{\Delta T}(\hat{\mathbf{q}}')\rangle \equiv \sum_{l=0}^{\infty}\frac{(2l+1)}{4\pi}\,C_l\;W_l(\hat{\mathbf{q}},\,\hat{\mathbf{q}}')\,, \tag{2.9}$$

where C_l is the angular power spectrum of CMB anisotropy signal and the window function

$$W_l(\hat{\mathbf{q}}_1,\hat{\mathbf{q}}_2) \;\equiv\; \int d\Omega_{\hat{\mathbf{q}}}\int d\Omega_{\hat{\mathbf{q}}'}\,B(\hat{\mathbf{q}}_1,\hat{\mathbf{q}})B(\hat{\mathbf{q}}_2,\hat{\mathbf{q}}')P_l(\hat{\mathbf{q}}\cdot\hat{\mathbf{q}}'), \tag{2.10}$$

encodes the effect of finite resolution through the beam function. A CMB anisotropy experiment probes a range of angular scales characterized by a *window* function $W_l(\hat{\mathbf{q}},\hat{\mathbf{q}}')$. The window depends both on the scanning strategy as well as the angular resolution and response of the experiment. However, it is neater to logically separate these two effects by expressing the window $W_l(\hat{\mathbf{q}},\hat{\mathbf{q}}')$ as a sum of 'elementary' window function of the CMB anisotropy [30]. For a given scanning strategy, the results can be readily generalized using the representation of the window function as sum over elementary window functions (see, *e.g.,* [30, 34]).

For some experiments, the beam function may be assumed to be circularly symmetric about the pointing direction, i.e., $B(\hat{\mathbf{q}},\hat{\mathbf{q}}') \equiv B(\hat{\mathbf{q}}\cdot\hat{\mathbf{q}}')$ without significantly affecting the results of the analysis. In any case, this assumption allows a great simplification since the beam function can then be represented by an expansion in Legendre polynomials as

$$B(\hat{\mathbf{q}}\cdot\hat{\mathbf{q}}') \;=\; \frac{1}{4\pi}\sum_{l=0}^{\infty}(2l+1)\,B_l\,P_l(\hat{\mathbf{q}}\cdot\hat{\mathbf{q}}'). \tag{2.11}$$

Consequently, it is straightforward to derive the well known simple expression

$$W_l(\hat{\mathbf{q}},\,\hat{\mathbf{q}}') \;=\; B_l^2\,P_l(\hat{\mathbf{q}}\cdot\hat{\mathbf{q}}')\,, \tag{2.12}$$

for a circularly symmetric beam function. The Pseudo-C_l estimator

$$\widetilde{C}_l \;\equiv\; \frac{1}{2l+1}\sum_{m=-l}^{l}|\widetilde{a}_{lm}|^2\,, \tag{2.13}$$

takes the form

$$\widetilde{C}_l \;=\; \frac{1}{4\pi}\int_{4\pi}d\Omega_{\hat{\mathbf{q}}_1}\int_{4\pi}d\Omega_{\hat{\mathbf{q}}_2}\,U(\hat{\mathbf{q}}_1)\,U(\hat{\mathbf{q}}_2)\,P_l(\hat{\mathbf{q}}_1\cdot\hat{\mathbf{q}}_2)\,\widetilde{\Delta T}(\hat{\mathbf{q}}_1)\,\widetilde{\Delta T}(\hat{\mathbf{q}}_2), \tag{2.14}$$

for non-circular beams and incomplete sky coverage. In this case, the expectation value of the Pseudo-C_l estimator becomes

$$\langle\widetilde{\mathcal{C}}_l\rangle \;=\; \sum_{l'}A_{ll'}C_{l'} \;+\; \bar{C}_l^N, \tag{2.15}$$

that is, the estimator is non-trivially biased, where the *bias matrix* $A_{ll'}$ takes the form

$$A_{ll'} = \frac{1}{2l+1}\sum_{n=-l}^{l}\sum_{m=-l'}^{l'}\left|\int_{4\pi}d\Omega_{\hat{\mathbf{q}}}U(\hat{\mathbf{q}})\,Y_{ln}(\hat{\mathbf{q}})\left[\int_{4\pi}d\Omega_{\hat{\mathbf{q}}'}\,Y^*_{l'm}(\hat{\mathbf{q}}')\,B(\hat{\mathbf{q}},\hat{\mathbf{q}}')\right]\right|^2. \tag{2.16}$$

The noise term $\bar{C}_l^N$, arising from instrumental noise, can be measured to a very high accuracy. If the noise term for full sky coverage C_l^N is known, it can be combined with the bias matrix for incomplete sky coverage $M_{ll'}$ [27] to obtain the noise power spectrum for cut-sky $\bar{C}_l^N$

$$\bar{C}_l^N \;=\; \sum_{l'}M_{ll'}\,C_{l'}^N, \tag{2.17}$$

where, $M_{ll'}$ is defined as

$$M_{ll'} \;=\; \frac{2l'+1}{4\pi}\sum_{l''=|l-l'|}^{l+l'}(2l''+1)\begin{pmatrix} l & l' & l'' \\ 0 & 0 & 0\end{pmatrix}^2\mathcal{U}_{l''}. \tag{2.18}$$

Computation of the bias matrix is important for defining the unbiased Pseudo-C_l estimator

$$\widetilde{C}_l^{\rm UB} \;\equiv\; \sum_{l'}[A^{-1}]_{ll'}\left(\widetilde{C}_{l'} \;-\; \sum_{l''} M_{l'l''}\,C_{l''}^N\right) \tag{2.19}$$

that removes the systematic effects of beam non-circularity and incomplete sky coverage.

The experimental beams in CMB experiments are mildly non-circular, and hence it makes sense to define Beam Distortion Parameters (BDP) $\beta_{lm}(\ll 1)$ so that we can calculate the result in a perturbative expansion of small parameter. The BDP $\beta_{lm} \equiv b_{lm}/b_{l0}$ is expressed in terms of

$$\begin{aligned} b_{lm} &\equiv \int_{4\pi} d\Omega_{\hat{\mathbf{q}}}\, Y^*_{lm}(\hat{\mathbf{q}})\, B(\hat{\mathbf{z}},\hat{\mathbf{q}})\,, \\ B_l &\equiv \int_{-1}^{1} d(\hat{\mathbf{q}}\cdot\hat{\mathbf{q}}')\, P_l(\hat{\mathbf{q}}\cdot\hat{\mathbf{q}}')\, \mathcal{B}(\hat{\mathbf{q}}\cdot\hat{\mathbf{q}}') \end{aligned} \tag{2.20}$$

where $\mathcal{B}(\hat{\mathbf{q}}\cdot\hat{\mathbf{q}}')$ is the *circularized* beam obtained by averaging $B(\hat{\mathbf{z}},\hat{\mathbf{q}})$ over azimuth ϕ. Hence,

$$B_l = \int_0^{\pi} \sin\theta d\theta \sqrt{\frac{4\pi}{2l+1}}\, Y^*_{l0}(\hat{\mathbf{q}}) \left[\frac{1}{2\pi}\int_0^{2\pi} d\phi\, B(\hat{\mathbf{z}},\hat{\mathbf{q}})\right] = \sqrt{\frac{4\pi}{2l+1}}\, b_{l0}. \tag{2.21}$$

Evaluation of the spherical harmonic transforms of the beam function $B(\hat{\mathbf{q}},\hat{\mathbf{q}}')$ for each pointing direction $\hat{\mathbf{q}}$ is computationally prohibitive. We use the spherical harmonic transforms b_{lm} of $B(\hat{\mathbf{z}},\hat{\mathbf{q}}')$, incorporating rotation in it via Wigner-D functions, in order to compute the harmonic transforms of $B(\hat{\mathbf{q}},\hat{\mathbf{q}}')$ for any $\hat{\mathbf{q}}$ from the formula [30]

$$\int_{4\pi} d\Omega_{\hat{\mathbf{q}}'}\, Y^*_{l'm}(\hat{\mathbf{q}}')\, B(\hat{\mathbf{q}},\hat{\mathbf{q}}') \;=\; \sqrt{\frac{2l'+1}{4\pi}} \sum_{m'=-l'}^{l'} B_{l'}\,\beta_{l'm'}\, D^{l'}_{mm'}(\hat{\mathbf{q}},\rho(\hat{\mathbf{q}})). \tag{2.22}$$

Using the spherical harmonic expansion of the mask function $U(\hat{\mathbf{q}})$

$$U(\hat{\mathbf{q}}) \;=\; \sum_{l=0}^{\infty}\sum_{m=-l}^{l} U_{lm}\, Y_{lm}(\hat{\mathbf{q}}) \tag{2.23}$$

we can rewrite the general form of the bias matrix [Eq. (2.16)] as

$$A_{ll'} \;=\; \frac{B_l^2}{4\pi}\frac{(2l'+1)}{(2l+1)} \sum_{n=-l}^{l}\sum_{m=-l'}^{l'} \left| \sum_{m'=-l'}^{l'} \beta_{l'm'} \sum_{l''=0}^{\infty}\sum_{m''=-l''}^{l''} U_{l''m''}\, J^{ll''l'}_{nm''mm'} \right|^2, \tag{2.24}$$

where

$$J^{ll''l'}_{nm''mm'} \;\equiv\; \int_{4\pi} d\Omega_{\hat{\mathbf{q}}}\, Y_{ln}(\hat{\mathbf{q}})\, Y_{l''m''}(\hat{\mathbf{q}})\, D^{l'}_{mm'}(\hat{\mathbf{q}},\rho(\hat{\mathbf{q}})). \tag{2.25}$$

To proceed further, we need a model for $\rho(\hat{\mathbf{q}})$. We shall proceed analytically assuming *"non-rotating"* beams, i.e. $\rho(\hat{\mathbf{q}}) = 0$. We evaluate the integral $J^{ll''l'}_{nm''mm'}$ using two different approaches. In the first method, using only the sinusoidal expansion of Wigner-d, we get (see Appendix A 1 and E for details)

$$\begin{aligned} J^{ll''l'}_{nm''mm'} \;=\; & 2\pi\,\delta_{(m-n)m''}\,(-1)^m\,\frac{\sqrt{(2l+1)(2l''+1)}}{4\pi} \;\times \\ & \sum_{M=-l}^{l} d^l_{nM}\left(\frac{\pi}{2}\right) d^l_{M0}\left(\frac{\pi}{2}\right) \sum_{M''=-l''}^{l''} d^{l''}_{(m-n)M''}\left(\frac{\pi}{2}\right) d^{l''}_{M''0}\left(\frac{\pi}{2}\right) \;\times \\ & \sum_{M'=-l'}^{l'} d^{l'}_{mM'}\left(\frac{\pi}{2}\right)\, d^{l'}_{M'm'}\left(\frac{\pi}{2}\right)\, f(m';M+M'+M''). \end{aligned} \tag{2.26}$$

where,

$$f(m';N) \equiv \begin{cases} (-1)^{(m'\pm1)/2}\,\pi/2 & \text{if } m' = odd \text{ and } N = \pm 1 \\ (-1)^{m'/2}\,2/(1-N^2) & \text{if both } m', N = 0 \text{ or } even \\ 0 & \text{otherwise.} \end{cases} \quad (2.27)$$

In the alternative method using Clebsch Gordon coefficients along with sinusoidal expansion of Wigner-d (see Appendix A 2 and E for details), we can evaluate $J^{ll''l'}_{nm''mm'}$ as:

$$\begin{aligned} J^{ll''l'}_{nm''mm'} &= (-1)^{n+m''}\,\delta_{m''(m-n)}\,\frac{\sqrt{(2l+1)(2l''+1)}}{2} \times \\ &\sum_{L=|l-l''|}^{l+l''} C^{L0}_{l0l''0}\,C^{L(n+m'')}_{lnl''m''} \sum_{L'=|L-l'|}^{L+l'} C^{L'(m-n-m'')}_{L(-n-m'')l'm}\,C^{L'm'}_{L0l'm'} \times \\ &\sum_{N=-L'}^{L'} d^{L'}_{0N}\left(\frac{\pi}{2}\right) d^{L'}_{Nm'}\left(\frac{\pi}{2}\right) f(m';N). \end{aligned} \quad (2.28)$$

The analytic expressions reduce to the known analytical results for circular beam and non-uniform sky coverage studied in ref. [27] and our earlier results for non-circular beam for full sky [29].

III. LIMITING CASES: CIRCULAR BEAM WITH FULL SKY COVERAGE & INCOMPLETE SKY COVERAGE

The special cases of circular beam and complete sky coverage limits are readily recovered from our general expressions.

First, the simplest case of complete sky coverage with circular beam limit can be obtained by substituting $U_{lm} = \sqrt{4\pi}\delta_{l0}$ and $\beta_{lm} = \delta_{m0}$. We show in the Appendix B 1 that we get back the well known result

$$A_{ll'} = B_l^2\,\delta_{ll'}. \quad (3.1)$$

Hivon et al.[27] formulated MASTER (Monte Carlo Apodized Spherical Transform Estimator) method for the estimation of CMB angular power spectrum from 'cut' (incomplete) sky coverage for circular beams cut sky. Substituting the circular beam limit [$\beta_{lm} = \delta_{m0}$] in the expression for bias matrix we recover the MASTER circular beam result in Appendix B 2:

$$A_{ll'} = B_l^2\,\frac{2l'+1}{4\pi} \sum_{l''=|l-l'|}^{l+l'} (2l''+1) \begin{pmatrix} l & l' & l'' \\ 0 & 0 & 0 \end{pmatrix}^2 \mathcal{U}_{l''}, \quad (3.2)$$

where $\mathcal{U}_{l''} \equiv \sum_{m''=-l''}^{l''} |U_{l''m''}|^2/(2l''+1)$.

Finally, in Appendix B 3, we recover the general formula for full sky coverage with non-circular beams presented in [29]. We substitute $U_{lm} = \sqrt{4\pi}\delta_{l0}$ in the expression for the bias matrix and get back

$$A_{ll'} = B_l^2\,\frac{(2l'+1)}{4} \sum_{m=-\min(l,l')}^{\min(l,l')} \left| \sum_{m'=-l'}^{l'} \beta_{l'm'} \int_{-1}^{1} d\cos\theta\, d^l_{m0}(\theta)\, d^{l'}_{mm'}(\theta) \right|^2. \quad (3.3)$$

Note that due to a somewhat different definition of bias matrix in [29], for $\mathcal{C}_l \equiv [l(l+1)/(8\pi^2)]C_l$, the results differ by a factor of $[l'(l'+1)]/[l(l+1)]$ from Eq (38) of [29]. Unfortunately, the complex form of leading order correction in the final expression for leading order correction to bias matrix presented in Eq (43) of [29], does not allow an explicit comparison of the results term by term.

IV. NUMERICAL IMPLEMENTATIONS

A. Fast computation of the bias matrix

The main motivation for deriving analytic results is to evade the computational cost and time taken estimating the bias using end to end simulations. The complexity is also apparent in the computationally prohibitive nature of the

four hierarchical integrals over the 2-spheres in the expression for the bias matrix. However, even the computation of the algebraic expression for the bias matrix in Section II is a significant computational challenge. A detailed numerical implementation has been proposed in this section.

The final analytic form of the bias matrix contains infinite summations. These summations have to be truncated for given accuracy goals using reasonable physical insights. Let us denote the (l, m) cut-offs for the mask and beam by $(l_{\rm mask}, m_{\rm mask})$ and $(l_{\rm beam}, m_{\rm beam})$ respectively. The choice of the numerical values for these cut-offs will be provided in the numerical results section.

Calculation of the final expression naively implementing the analytic expression given by Eqs (2.24) & (2.26), is computationally expensive. Three major innovations have been introduced in order to numerically evaluate the bias matrix:

1. We used a smart implementation of the hierarchical summations to reduce the computation cost by a few orders of magnitude. To calculate three coupled loops of the form

$$S = \sum_{i=1}^{N}\sum_{j=1}^{N}\sum_{k=1}^{N} f(i+j+k), \tag{4.1}$$

apparently N^3 operations are necessary. However, if we calculate the summation in the following order:

$$V(m) \;:=\; \sum_{k=1}^{N} f(m+k); \quad m = 1, 2, \ldots, 2N \tag{4.2}$$

$$S \;=\; \sum_{i=1}^{N}\sum_{j=1}^{N} V(i+j) \tag{4.3}$$

we effectively require just $2N^2 + N^2 = 3N^2$ operations. The computational gain is $N/3$. For $N = 900$, this factor is 300. This example is for a very simple case where all the summations have the same limits, but clearly this can be extended to the case of summations with unequal limits and match our analysis (See Appendix C for details).

In our analysis the summations within the modulus symbols in Eqs (2.24) & (2.26) (that is for each pair of m, n) are computed in three stages:

- Step I:

$$V_1(N) \;=\; \sum_{M'=-l'}^{l'} d^{l'}_{mM'}\left(\frac{\pi}{2}\right) \sum_{m'=-m_{\rm beam}}^{m_{\rm beam}} \beta_{l'm'}\, d^{l'}_{M'm'}\left(\frac{\pi}{2}\right)\, f(m'; M'+N) \tag{4.4}$$

  N runs from $-(l + m_{\rm mask})$ to $+(l + m_{\rm mask})$

- Step II:

$$V_2(M'') \;=\; \sum_{M=-l}^{l} d^{l}_{nM}\left(\frac{\pi}{2}\right)\, d^{l}_{M0}\left(\frac{\pi}{2}\right)\, V^1(M+M'') \tag{4.5}$$

- Step III:

$$V_3 \;=\; \sum_{l''=0}^{l_{\rm mask}} \sqrt{2l''+1}\, U_{l''(m-n)} \;\times \sum_{M''=-m_{\rm mask}}^{m_{\rm mask}} d^{l''}_{(m-n)M''}\left(\frac{\pi}{2}\right) d^{l''}_{M''0}\left(\frac{\pi}{2}\right) V^2(M'') \tag{4.6}$$

For $l_{\rm beam} = l_{\rm max}$ the above algorithm reduces the computation cost from $\sim (8/3)(2m_{\rm mask}+1)(2m_{\rm beam}+1)l^5_{\rm max}l^2_{\rm mask}$ to $\sim (4/3)(2m_{\rm mask}+1)(2m_{\rm beam}+1)l^5_{\rm max}$, providing a speed-up factor of $\sim 2l^2_{\rm mask}$.

Mildly non-circular beams, where the BDP β_{lm} at each l falls off rapidly with m, allows us to neglect β_{lm} for $m > m_{\rm beam}$. For most realistic beams, $m_{\rm beam} \sim 4$ is a sufficiently good approximation [30] and this cuts off the summation over BDP in the bias matrix $A_{ll'}$.

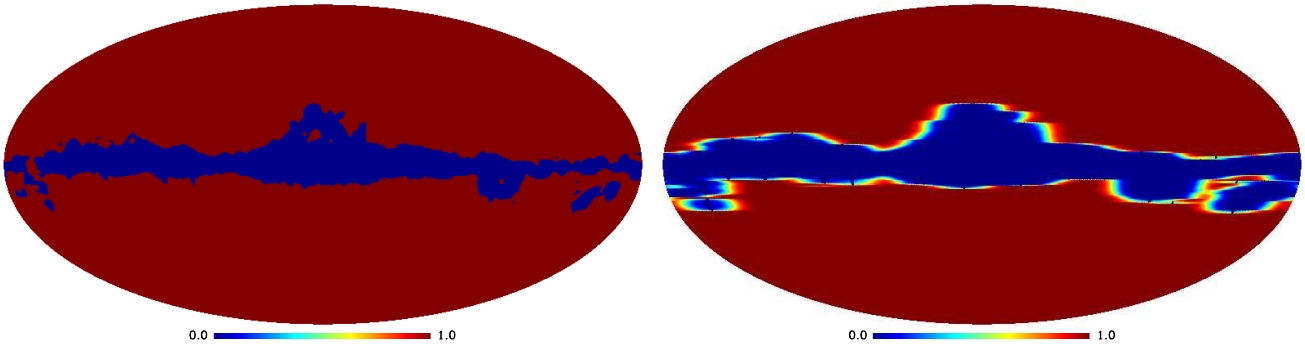

FIG. 2: The KP2 original mask (left) and the azimuthally smoothed mask reconstructed from the KP2 mask (right).

Soft, azimuthally apodized, masks where the coefficients U_{lm} are small beyond $m > m_{\rm mask}$. Moreover, it is useful to smooth the mask in l, such the U_{lm} die off rapidly for $l > l_{\rm mask}$ too.

Clearly, small values of $m_{\rm beam}$ and $m_{\rm mask}$ lead to computational speed up. Detailed discussion on mask making is shown in section IV B.

2. The Wigner-d functions with argument $\pi/2$ occur too frequently in the above evaluation. So one possibility to reduce computation cost was to pre-compute all the Wigner-d coefficients $d^l_{mn}(\pi/2)$ at once. But for $l \sim 1000$ this scheme is limited by disk/memory storage and/or program Input/Output (I/O) overhead.

   However, we may observe that, in each step of computation described in Eq (4.6) only one value of l occurs in the d symbols. Hence we use an efficient recursive routine presented in [35] that generates all the $d^l_{mn}(\pi/2)$ at once for a given value of l. This allows us to compute the Wigner-d symbols efficiently and use them as constant co-efficients at each step without any significant I/O limited operations.

3. Finally, we expect that the bias matrix is not far off from diagonal, because the beams are mildly non-circular. So we need not compute all the elements of the bias matrix. Rather, a diagonal band (triangular shape) of average "thickness" Δl can be used to calculate the C_l estimation error with a fairly high accuracy. This will give an additional speed-up factor of $\sim l/\Delta l$.

B. Constructing azimuthally apodized masks

The temperature anisotropies observed by any detector are combinations of CMB as well as foreground. The dominant contribution of foreground arises from the galactic plane. While methods of foreground removal using multi-wavelength observations exist, there is significant residual along the galactic plane to require masking of that region prior to cosmological power spectrum estimation. The mask is designed to remove the effect of regions of excessive galactic emission and spots around strong extragalactic radio sources.

The effect of masked map on the angular power spectrum estimation has been described in the literature[27]. However, as we have shown, the effect of cut sky becomes nontrivial for a non-circular beam function. The sum over all the U_{lm} modes of the mask is responsible for the large additional computation cost. In particular, our computational cost estimate in the previous subsection shows that a mask that allows us to choose a modest value of $m_{\rm mask}$ leads to a proportionally smaller computational cost. A mask whose transform is such that power in high m modes for a given l is suppressed would clearly serve this purpose.

To achieve this we propose a possible method for generating an azimuthally-apodized version of a given mask [49] as outlined in the following steps:

1. We compute spherical harmonic coefficients U_{lm} of the original mask $U^o(\hat{q})$. We directly suppress the power at high m, by rescaling

$$U'_{lm} = e(-m * m/[\alpha\, {m_{\rm mask}}^2]) * U_{lm} \tag{4.7}$$

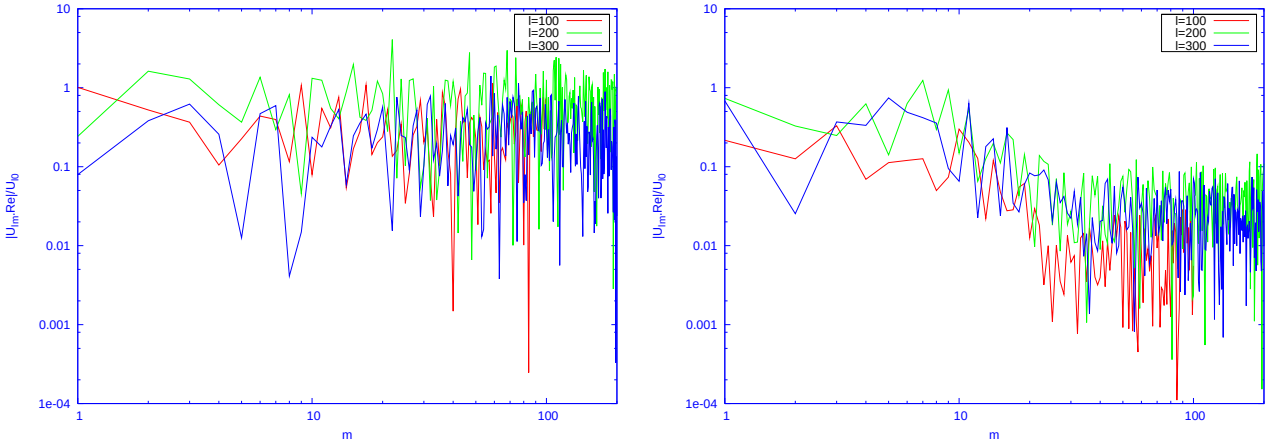

FIG. 3: U_{lm}s of the original mask KP2 (left) and the mask Kp2′ (right).

corresponding to smoothing the mask along the azimuthal direction. Where α determines the extent to which power is suppressed at the given cut-off value of $m_{\rm mask}$.

2. The rescaled U_{lm} are transformed to make an auxiliary mask $U'(\hat{q})$.

3. However, it is clear that mask $U'(\hat{q})$ would allow power from contaminated regions. We should ensure that all regions where $U^o(\hat{q}) = 0$ remain zero. A simple way to do that would be to multiply $U'(\hat{q})$ with $U^o(\hat{q})$ in the pixel space. Hence, we define the final apodized mask as

$$U^a(\hat{q}) = U'(\hat{q})[U^o(\hat{q})]^s \tag{4.8}$$

where s is a sufficiently large number ($s = 12$ in our example shown in figures 2 & 3) to ensure that the edges of the final mask are smoothed to the required level.

The final mask obtained in this method is shown in the right panel of figure 2. We extract U_{lm} from this final mask $U^a(\hat{q})$. We show the U_{lm} of the original mask KP2 and the azimuthally apodized mask Kp2^a in figure 3. Clearly, the later show very rapid decrease of a mode with m for a given l. In the example shown here, we have significant contribution only from the first 10-20 m modes, for a given l. The $|U_{lm}|^2$ also dies down with l allowing us also to put a cut-off at $l = l_{\rm mask} \sim 100$. A reconstructed mask following this method has the advantage that it reduces the computation time for bias matrix by a large factor.

V. DISCUSSIONS

The assumption of non-circular beam leads to major complications at every stage of the data analysis pipeline. The extent to which the non-circularity affects the step of going from the time-stream data to sky map is very sensitive to the scan-strategy. The beam now has an orientation with respect to the scan path that can potentially vary along the path. This implies that the beam function is inherently time dependent and difficult to deconvolve.

In our present work, we have extended our analytic approach for addressing the effect of non-circular experimental beam function in the estimation of the angular power spectrum C_l of CMB anisotropy, which also includes the effect of incomplete sky coverage. Non-circular beam effects can be modeled into the covariance functions in approaches related to maximum likelihood estimation [8, 9] and can also be included in the Harmonic ring [15] and ring-torus estimators [16]. However, all these methods are computationally prohibitive for high resolution maps and, at present, the computationally economical approach of using a Pseudo-C_l estimator appears to be a viable option for extracting the power spectrum at high multipoles [3]. The Pseudo-C_l estimates have to be corrected for the systematic biases. While considerable attention has been devoted to the effects of incomplete/non-uniform sky coverage, no comprehensive or systematic approach is available for non-circular beam. The high sensitivity, 'full' (large) sky observation from space (long duration balloon) missions have alleviated the effect of incomplete sky coverage and other systematic effects such as the one we consider here have gained more significance. Non-uniform coverage, in particular, the galactic masks affect only CMB power estimation at the low multipoles. The analysis accompanying the recent second data release

from WMAP uses the hybrid strategy [3] where the power spectrum at low multipoles is estimated using optimal Maximum Likelihood methods and Pseudo-C_l are used for large multipoles [32, 42].

The non-circular beam is an effect that dominates at large l beyond the the inverse beam width [29]. For high resolution experiments, the optimal maximum likelihood methods which can account for non-circular beam functions are computationally prohibitive. In implementing the Pseudo-C_l estimation, we have included both the non-circular beam effect and the effect of non-uniform sky coverage. Our work provides a convenient approach for estimating the magnitude of these effects in terms of the leading order deviations from a circular beam and azimuthally symmetric mask. The perturbative approach is very efficient. For most CMB experiments the leading few orders capture most of the effect of beam non-circularity [30]. Our results highlight the advantage of azimuthally smoothed masks (mild deviations from azimuthal symmetry) in reducing computational costs. This process is more efficient as compared to the isotropic apodization of masks[36], that suffers a lot more information loss at the edges. The numerical implementation of our method can readily accommodate the case when pixels are revisited by the beam with different orientations. Evaluating the realistic bias and error-covariance for a specific CMB experiment with non-circular beams would require numerical evaluation of the general expressions for $A_{ll'}$ using real scan strategy and account for inhomogeneous noise and sky coverage, the latter part of which has been addressed in this present work.

It is worthwhile to note in passing that that the angular power C_l contains all the information of Gaussian CMB anisotropy only under the assumption of statistical isotropy. Gaussian CMB anisotropy map measured with a non-circular beam corresponds to an underlying correlation function that violates statistical isotropy. In this case, the extra information present may be measurable using, for example, the bipolar power spectrum [38, 43, 44, 45]. Even when the beam is circular the scanning pattern itself is expected to cause a breakdown of statistical isotropy of the measured CMB anisotropy [27]. For a non-circular beam, this effect could be much more pronounced and, perhaps, presents an interesting avenue of future study.

In addition to temperature fluctuations, the CMB photons coming from different directions have a random, linear polarization. The polarization of CMB can be decomposed into E part with even parity and B part with odd parity. Besides the angular spectrum C_l^{TT}, the CMB polarization provides three additional spectra, C_l^{TE}, C_l^{EE} and C_l^{BB} which are invariant under parity transformations. The level of polarization of the CMB being about a tenth of the temperature fluctuation, it is only very recently that the angular power spectrum of CMB polarization field has been detected. The Degree Angular Scale Interferometer (DASI) has measured the CMB polarization spectrum over limited band of angular scales in late 2002 [39]. The DASI experiment recently published 3-year results of much refined measurements [46]. More recently, the BOOMERanG collaboration reported new measurements of CMB anisotropy and polarization spectra [47]. The WMAP mission has also measured CMB polarization spectra [40, 48]. Correcting for the systematic effects of a non-circular beam for the polarization spectra is expected to become important. Extending this work to the case CMB polarization is another line of activity we plan to undertake in the near future.

In summary, we have presented a perturbation framework to compute the effect of non-circular beam function on the estimation of power spectrum of CMB anisotropy taking into account the effect of a non-uniform sky coverage (eg., galactic mask). We not only present the most general expression including non-uniform sky coverage as well as a non-circular beam that can be numerically evaluated but also provide elegant analytic results in interesting limits. As CMB experiments strive to measure the angular power spectrum with increasing accuracy and resolution, the work provides a stepping stone to address a rather complicated systematic effect of non-circular beam functions.

APPENDIX A: EVALUATION OF $J^{ll''l'}_{nm''mm'}$

Evaluation of $J^{ll''l'}_{nm''mm'}$ in Eq. (2.24) can be done, deploying two procedures. In the first, we use purely sinusoidal expansion of the Wigner-d, whereas for the second, we use the Clebsch-Gordon coefficients along with the Wigner-d.

1. Using the sinusoidal expansion of the Wigner-d

In the first process, we start by pluging in Eq. (D15) in Eq. (2.25)

$$\begin{aligned} J^{ll''l'}_{nm''mm'} &:= \int_{4\pi} d\Omega_{\hat{\mathbf{q}}}\, Y_{ln}(\hat{\mathbf{q}})\, Y_{l''m''}(\hat{\mathbf{q}})\, D^{l'}_{mm'}(\hat{\mathbf{q}}, \rho(\hat{\mathbf{q}})) \\ &= \frac{\sqrt{(2l+1)(2l''+1)}}{4\pi} \int_0^{2\pi} d\phi\, e^{i(n+m''-m)\phi} \;\times \end{aligned}$$

$$
\begin{aligned}
&\int_0^\pi \sin\theta d\theta\, d^l_{n0}(\theta)\, d^{l''}_{m''0}(\theta)\, d^{l'}_{mm'}(\theta)\, e^{-im'\rho(\hat{\mathbf{q}})} \\
&= \frac{\sqrt{(2l+1)(2l''+1)}}{4\pi}\, i^{n+m+m'+m''} \sum_{M=-l}^{l} d^l_{nM}\left(\frac{\pi}{2}\right) d^l_{M0}\left(\frac{\pi}{2}\right) \times \\
&\sum_{M''=-l''}^{l''} d^{l''}_{m''M''}\left(\frac{\pi}{2}\right) d^{l''}_{M''0}\left(\frac{\pi}{2}\right) \sum_{M'=-l'}^{l'} d^{l'}_{mM'}\left(\frac{\pi}{2}\right) d^{l'}_{M'm'}\left(\frac{\pi}{2}\right) \times \\
&(-1)^{M+M''+M'} \int_0^{2\pi} d\phi\, e^{i(n+m''-m)\phi} \int_0^\pi \sin\theta d\theta\, e^{i(M+M'+M'')\theta}\, e^{-im'\rho(\hat{\mathbf{q}})}. \qquad \text{(A1)}
\end{aligned}
$$

To proceed further *analytically*, we need a model for $\rho(\hat{\mathbf{q}})$. We shall assume *non-rotating* beams approximation where the scan pattern is such that $\rho(\hat{\mathbf{q}}) = 0$. In this case the ϕ integral above is separable. Using,

$$
\int_0^{2\pi} d\phi\, e^{i(n+m''-m)\phi} \;=\; 2\pi\, \delta_{m''(m-n)} \qquad \text{(A2)}
$$

we can get a simplified result:

$$
\begin{aligned}
J^{ll''l'}_{nm''mm'} \;&=\; 2\pi\, \delta_{m''(m-n)} \frac{\sqrt{(2l+1)(2l''+1)}}{4\pi} \sum_{M=-l}^{l} d^l_{nM}\left(\frac{\pi}{2}\right) d^l_{M0}\left(\frac{\pi}{2}\right) \;\times \\
&\sum_{M''=-l''}^{l''} d^{l''}_{m''M''}\left(\frac{\pi}{2}\right) d^{l''}_{M''0}\left(\frac{\pi}{2}\right) \sum_{M'=-l'}^{l'} d^{l'}_{mM'}\left(\frac{\pi}{2}\right) d^{l'}_{M'm'}\left(\frac{\pi}{2}\right) \times \\
&\left[i^{n+m+m'+m''}\, (-1)^{M+M''+M'} \int_0^\pi \sin\theta d\theta\, e^{i(M+M'+M'')\theta} \right]. \qquad \text{(A3)}
\end{aligned}
$$

The above expression is real. The proof is given below:

Contribution for all of $M, M', M'' = 0$:

For this term the integral of the above expression is real. Therefore, if $n + m + m' + m'' = even$ this term is real (because then the factor $i^{n+m+m'+m''}$ is real). When $n + m + m' + m'' = odd$, which means at least one of $n, m + m', m''$ is odd, this term does not contribute, since $d^l_{m0}(\pi/2) d^l_{0m'}(\pi/2) = 0$ if $m + m' = odd$ (follows from Eq. (6) of §4.16 of [41]).

Contribution for *not* all of $M, M', M'' = 0$:

For each set of M, M', M'' in the above summation, there exists a set $-M, -M', -M''$, which converts the integral of the above expression to its complex conjugate. Since $d^l_{mm'}(\pi/2) = (-1)^{l-m'} d^l_{-mm'}(\pi/2)(-1)^{l+m} d^l_{m-m'}(\pi/2)$ (see Eq. (1) of §4.4 of [41]), the Wigner-d symbols give a factor of $(-1)^{n+m+m'+m''}$. So, if $n + m + m' + m'' = even$, the sum is real, as well as the factor $i^{n+m+m'+m''}$ and both are imaginary if $n + m + m' + m'' = odd$.

Therefore, the full summation is always real.

Following the discussion on the reality of the expression and using Eq. (E8) we can write

$$
\begin{aligned}
J^{ll''l'}_{nm''mm'} \;&=\; 2\pi\, \delta_{(m-n)m''}\, (-1)^m \frac{\sqrt{(2l+1)(2l''+1)}}{4\pi} \;\times \\
&\sum_{M=-l}^{l} d^l_{nM}\left(\frac{\pi}{2}\right) d^l_{M0}\left(\frac{\pi}{2}\right) \sum_{M''=-l''}^{l''} d^{l''}_{(m-n)M''}\left(\frac{\pi}{2}\right) d^{l''}_{M''0}\left(\frac{\pi}{2}\right) \;\times \\
&\sum_{M'=-l'}^{l'} d^{l'}_{mM'}\left(\frac{\pi}{2}\right) d^{l'}_{M'm'}\left(\frac{\pi}{2}\right) f(m'; M + M' + M''). \qquad \text{(A4)}
\end{aligned}
$$

Moreover, since for "symmetric" beams $\beta_{lm} = 0$ for $m = odd$, in the final expression terms with $m' = odd$ shall not contribute, that means, *for symmetric beams*, $f(m'; N)$ contributes *only* when both $m', N = 0$ or *even*.

To make the final expression simpler, we can write the bias matrix for non-rotating beam with incomplete sky coverage as:

$$\begin{aligned} A_{ll'} \;=\; & B_l^2\,\frac{(2l'+1)}{16\pi}\sum_{n=-l}^{l}\sum_{m=-l'}^{l'}\left|\sum_{l''=0}^{\infty}\sqrt{2l''+1}\,U_{l''(m-n)}\;\times\right. \\ & \sum_{M''=-l''}^{l''} d^{l''}_{(m-n)M''}\left(\frac{\pi}{2}\right)\,d^{l''}_{M''0}\left(\frac{\pi}{2}\right)\sum_{M=-l}^{l} d^{l}_{nM}\left(\frac{\pi}{2}\right)\,d^{l}_{M0}\left(\frac{\pi}{2}\right)\;\times \\ & \left.\sum_{M'=-l'}^{l'} d^{l'}_{mM'}\left(\frac{\pi}{2}\right)\sum_{m'=-l'}^{l'}\beta_{l'm'}\,d^{l'}_{M'm'}\left(\frac{\pi}{2}\right)\,f(m';M+M'+M'')\right|^2. \end{aligned} \tag{A5}$$

This form is useful for numerical evaluation.

2. Using Clebsch-Gordon series and expansion of Wigner-d

Putting Eq (E6), (E4), (E2), (E5) & (D15) in Eq (2.24) we get

$$\begin{aligned} J^{ll''l'}_{nm''mm'} \;\equiv\; & \int_{4\pi} d\Omega_{\hat{\mathbf{q}}}\,Y_{ln}(\hat{\mathbf{q}})\,Y_{l''m''}(\hat{\mathbf{q}})\,D^{l'}_{mm'}(\hat{\mathbf{q}},\rho(\hat{\mathbf{q}})) \\ =\; & \sum_{L=|l-l''|}^{l+l''}\sqrt{\frac{(2l+1)(2l''+1)}{4\pi(2L+1)}}\,C^{L0}_{l0l''0}\,C^{L(n+m'')}_{lnl''m''}\;\times \\ & \int_{4\pi} d\Omega_{\hat{\mathbf{q}}}\,Y_{L(n+m'')}(\hat{\mathbf{q}})D^{l'}_{mm'}(\hat{\mathbf{q}},\rho(\hat{\mathbf{q}})) \\ =\; & (-1)^{n+m''}\,\frac{\sqrt{(2l+1)(2l''+1)}}{4\pi}\times \\ & \sum_{L=|l-l''|}^{l+l''} C^{L0}_{l0l''0}C^{L(n+m'')}_{lnl''m''}\int_{4\pi} d\Omega_{\hat{\mathbf{q}}}D^{L}_{(-n-m'')0}(\hat{\mathbf{q}},\rho(\hat{\mathbf{q}}))D^{l'}_{mm'}(\hat{\mathbf{q}},\rho(\hat{\mathbf{q}})) \\ =\; & (-1)^{n+m''}\,\frac{\sqrt{(2l+1)(2l''+1)}}{4\pi}\sum_{L=|l-l''|}^{l+l''} C^{L0}_{l0l''0}\,C^{L(n+m'')}_{lnl''m''}\times \\ & \sum_{L'=|L-l'|}^{L+l'} C^{L'(m-n-m'')}_{L(-n-m'')l'm}\,C^{L'm'}_{L0l'm'}\int_{4\pi} d\Omega_{\hat{\mathbf{q}}}\,D^{L'}_{(m-n-m'')m'}(\hat{\mathbf{q}},\rho(\hat{\mathbf{q}})). \end{aligned} \tag{A6}$$

Now using Eq. (D15) one can write integrals of the above form as ($m - n - m'' \to M'$ & $m' \to M''$):

$$\begin{aligned} & \int_{4\pi} d\Omega_{\hat{\mathbf{q}}}\,D^{L'}_{M'M''}(\hat{\mathbf{q}},\rho(\hat{\mathbf{q}})) \;= \\ & i^{M'+M''}\sum_{N=-L'}^{L'}(-1)^N\,d^{L'}_{M'N}\left(\frac{\pi}{2}\right)\,d^{L'}_{NM''}\left(\frac{\pi}{2}\right)\int_{4\pi} d\Omega_{\hat{\mathbf{q}}}\,e^{-iM'\phi}\,e^{iN\theta}\,e^{-iM''\rho(\hat{\mathbf{q}})}. \end{aligned} \tag{A7}$$

To proceed further *analytically*, we need a model for $\rho(\hat{\mathbf{q}})$. We shall continue assuming *non-rotating* beams, i.e. $\rho(\hat{\mathbf{q}}) = 0$. In this case the ϕ integral above is separable. Then, putting Eq. (A2) we get

$$\begin{aligned} & \int_{4\pi} d\Omega_{\hat{\mathbf{q}}}\,D^{L'}_{M'M''}(\hat{\mathbf{q}},0) \;= \\ & 2\pi\,\delta_{M'0}\,i^{M''}\sum_{N=-L'}^{L'}(-1)^N\,d^{L'}_{0N}\left(\frac{\pi}{2}\right)\,d^{L'}_{NM''}\left(\frac{\pi}{2}\right)\int_0^{\pi}\sin\theta d\theta\,e^{iN\theta}. \end{aligned} \tag{A8}$$

This integral is real. This becomes clear if we write the right hand side of the above equation as

$$2\pi\delta_{M'0}i^{M''}\left[2\,d^{L'}_{00}\left(\frac{\pi}{2}\right)d^{L'}_{0M''}\left(\frac{\pi}{2}\right)+\sum_{N=1}^{L'}(-1)^N d^{L'}_{0N}\left(\frac{\pi}{2}\right)d^{L'}_{NM''}\left(\frac{\pi}{2}\right)\;\times\right.$$
$$\left.\int_0^\pi \sin\theta d\theta\left\{e^{iN\theta}+(-1)^{M''}e^{-iN\theta}\right\}\right]. \tag{A9}$$

When $M''=even$ both $i^{M''}$ and the integrand are real, and when $M''=odd$ both $i^{M''}$ and the integrand are imaginary. The first term inside the square bracket does not contribute when $M''=odd$ (since $d^{L'}_{00}(\pi/2)d^{L'}_{0M''}(\pi/2)$ vanishes in that case). Therefore irrespective of the value of M'' the above expression is real. Thus,

$$\int_{4\pi}d\Omega_{\hat{\mathbf{q}}}\,D^{L'}_{M'M''}(\hat{\mathbf{q}},0)\;= \tag{A10}$$
$$2\pi\,\delta_{M'0}\sum_{N=-L'}^{L'}d^{L'}_{0N}\left(\frac{\pi}{2}\right)d^{L'}_{NM''}\left(\frac{\pi}{2}\right)\Re\left[i^{M''}\,(-1)^N\int_0^\pi\sin\theta d\theta\,e^{iN\theta}\right].$$

Now we can use the above results and combine with Eq. (E8) to get

$$J^{ll''l'}_{nm''mm'}\;=\;(-1)^{n+m''}\,\delta_{m''(m-n)}\,\frac{\sqrt{(2l+1)(2l''+1)}}{2}\;\times$$
$$\sum_{L=|l-l''|}^{l+l''}C^{L0}_{l0l''0}\,C^{L(n+m'')}_{lnl''m''}\sum_{L'=|L-l'|}^{L+l'}C^{L'(m-n-m'')}_{L(-n-m'')l'm}\,C^{L'm'}_{L0l'm'}\;\times$$
$$\sum_{N=-L'}^{L'}d^{L'}_{0N}\left(\frac{\pi}{2}\right)d^{L'}_{Nm'}\left(\frac{\pi}{2}\right)\,f(m';N). \tag{A11}$$

The final form of the bias matrix for non-rotating beam with incomplete sky coverage can now be written as (after replacing m'' by $m-n$, pulling out few factors outside the modulus and squaring):

$$A_{ll'}\;=\;B_l^2\,\frac{(2l'+1)}{16\pi}\sum_{n=-l}^{l}\sum_{m=-l'}^{l'}\left|\sum_{l''=0}^{\infty}\sqrt{2l''+1}\,U_{l''(m-n)}\;\times\right.$$
$$\sum_{L=|l-l''|}^{l+l''}C^{L0}_{l0l''0}\,C^{Lm}_{lnl''(m-n)}\sum_{L'=|L-l'|}^{L+l'}C^{L'0}_{L-ml'm}\sum_{N=-L'}^{L'}d^{L'}_{0N}\left(\frac{\pi}{2}\right)\;\times$$
$$\left.\sum_{m'=-l'}^{l'}\beta_{l'm'}\,C^{L'm'}_{L0l'm'}\,d^{L'}_{Nm'}\left(\frac{\pi}{2}\right)\,f(m';N)\right|^2. \tag{A12}$$

APPENDIX B: CONSISTENCY CHECKS

1. The full sky and circular beam limit

In this we recover the special case of circular beam and complete sky coverage limit. From Eq. A12, the full sky limit $[U_{lm}\sqrt{4\pi}\delta_{l0}]$ is obtained by replacing $U_{l''(m-n)}$ with $\sqrt{4\pi}\delta_{l''0}\delta_{mn}$; and for the circular beam, we replace the BDP $\beta_{l'm'}$ with $\delta_{m'0}$. So,

$$A_{ll'}\;=\;B_l^2\,\frac{2l'+1)}{4}\sum_{n=-\min(l,l')}^{\min(l,l')}\left|C^{l0}_{l000}\,C^{ln}_{ln00}\sum_{L'=|l-l'|}^{l+l'}C^{L'0}_{l-nl'n}\,C^{L'0}_{l0l'0}\;\times\right.$$
$$\left.\sum_{N=-L'}^{L'}d^{L'}_{0N}\left(\frac{\pi}{2}\right)d^{L'}_{N0}\left(\frac{\pi}{2}\right)\,f(0;N)\right|^2. \tag{B1}$$

From the relation $C^{c\gamma}_{a\alpha 00} = \delta_{ac}\delta_{\alpha\gamma}$ (Eq. (2) in §8.5.1 of [41]), we can reduce C^{l0}_{l000} and C^{ln}_{ln00} to unity, and get:

$$A_{ll'} = B_l^2\,\frac{2l'+1}{4}\sum_{n=-\min(l,l')}^{\min(l,l')}\left|\sum_{L'=|l-l'|}^{l+l'} C^{L'0}_{l-nl'n}\,C^{L'0}_{l0l'0}\sum_{N=-L'}^{L'} d^{L'}_{0N}\left(\frac{\pi}{2}\right)d^{L'}_{N0}\left(\frac{\pi}{2}\right)\,f(0;N)\right|^2. \tag{B2}$$

To get the value of $\sum_{N=-L'}^{L'} d^{L'}_{0N}\left(\frac{\pi}{2}\right)d^{L'}_{N0}\left(\frac{\pi}{2}\right)f(0;N)$, we have to start a step back.

$$\begin{aligned} Y^*_{lm}(\hat{q}) &= \sqrt{\frac{2l+1}{4\pi}}D^l_{mm'}(\hat{q},0) \\ &= \sqrt{\frac{2l+1}{4\pi}}i^m e^{-im\phi}\sum_{N=-l}^{l}(-1)^N d^l_{mN}\left(\frac{\pi}{2}\right)d^l_{N0}\left(\frac{\pi}{2}\right)e^{iN\theta} \end{aligned} \tag{B3}$$

From the relation

$$\int_{4\pi} Y^*_{lm}(\hat{q})d\Omega_{\hat{q}}\sqrt{4\pi}\delta_{l0}\delta_{m0}$$

it follows that

$$\begin{aligned} &\sqrt{\frac{2l+1}{4\pi}}i^m\sum_{N=-l}^{l}(-1)^N d^l_{mN}\left(\frac{\pi}{2}\right)d^l_{N0}\left(\frac{\pi}{2}\right)\int e^{iN\theta}sin\theta d\theta\int e^{-im\phi}d\phi \\ &= \sqrt{4\pi}\delta_{l0}\delta_{m0}. \end{aligned} \tag{B4}$$

The last integral (i.e., $\int e^{-im\phi}d\phi$) gives $2\pi\delta_{m0}$. So, equating out both sides and rearranging, we have

$$i^m\sum_{N=-l}^{l}(-1)^N d^l_{mN}\left(\frac{\pi}{2}\right)d^l_{N0}\left(\frac{\pi}{2}\right)\int e^{iN\theta}sin\theta d\theta\int e^{-im\phi}d\phi = \frac{2}{\sqrt{2l+1}}\delta_{l0}. \tag{B5}$$

The l.h.s. is identified with the relation $\sum_{N=-L'}^{L'} d^{L'}_{0N}\left(\frac{\pi}{2}\right)d^{L'}_{N0}\left(\frac{\pi}{2}\right)f(0;N)$, and hence Eq.(B2) reduces to

$$\begin{aligned} A_{ll'} &= B_l^2\,\frac{2l'+1}{4}\sum_{n=max(-l,-l')}^{min(l,l')}\left|\sum_{L'=|l-l'|}^{l+l'} C^{L'0}_{l-nl'n}\,C^{L'0}_{l0l'0}\frac{2}{\sqrt{2L'+1}}\delta_{L'0}\right|^2 \\ &= B_l^2\,(2l'+1)\sum_{n=max(-l,-l')}^{min(l,l')}\left|C^{00}_{l-nl'n}\,C^{00}_{l0l'0}\right|^2. \end{aligned} \tag{B6}$$

We know from Eq. (1) of §8.5.1 of [41]

$$C^{00}_{a\alpha b\beta}(-1)^{a-\alpha}\frac{\delta_{ab}\delta_{\alpha,-\beta}}{\sqrt{2a+1}}.$$

Hence, $A_{ll'}$ finally reduces to the well known result

$$A_{ll'} = B_l^2\,\delta_{ll'}. \tag{B7}$$

2. The circular beam limit with incomplete sky coverage

We will show in this section that our formulation reduces to the analytic limit of the MASTER method of Hivon et al. [27] for the incomplete sky coverage taking circular beams. Following the procedure mentioned in §B 1, we proceed as:

$$\begin{aligned} A_{ll'} &= B_l^2\,\frac{2l'+1}{16\pi}\sum_{n=-l}^{l}\sum_{m=-l'}^{l'}\left|\sum_{l''=0}^{\infty}\sqrt{2l''+1}\,U_{l''(m-n)}\sum_{L=|l-l''|}^{l+l''} C^{L0}_{l0l''0}\,C^{Lm}_{lnl''(m-n)}\right. \\ &\left.\times\sum_{L'=|L-l'|}^{L+l'} C^{L'0}_{L-ml'm}\,C^{L'0}_{L0l'0}\sum_{N=-L'}^{L'} d^{L'}_{0N}\left(\frac{\pi}{2}\right)d^{L'}_{N0}\left(\frac{\pi}{2}\right)\,f(0;N)\right|^2. \end{aligned} \tag{B8}$$

Using Eq. (B5), we get

$$A_{ll'} = B_l^2 \frac{2l'+1}{4\pi} \sum_{n=-l}^{l} \sum_{m=-l'}^{l'} \times \left| \sum_{l''=0}^{\infty} \sqrt{2l''+1}\, U_{l''(m-n)} \sum_{L=|l-l''|}^{l+l''} C^{L0}_{l0l''0}\, C^{Lm}_{lnl''(m-n)} C^{00}_{L(-m)l'm}\, C^{00}_{L0l'0} \right|^2$$
$$= \frac{B_l^2}{4\pi} \sum_{n=-l}^{l} \sum_{m=-l'}^{l'} \left| \sum_{l''=0}^{\infty} \sqrt{2l''+1}\, U_{l''(m-n)} \sum_{L=|l-l''|}^{l+l''} C^{L0}_{l0l''0}\, C^{Lm}_{lnl''(m-n)} \right|^2$$

To arrive at Eq. A31 of Hivon et al. [27], we first replace $(m-n)$ by m'' and then open up the modulus square. The symbol $C^{l'm}_{lnl''m''}$ contributes only when m'' is equal to $(m-n)$ and also l'' satisfies the triangle inequality.

$$A_{ll'} = \frac{B_l^2}{4\pi\,(2l'+1)} \sum_{n=-l}^{l} \sum_{m=-l'}^{l'} \left| \sum_{l''=0}^{\infty} \sqrt{2l''+1} \sum_{m''=-l''}^{l''} U_{l''m''} C^{l'0}_{l0l''0}\, C^{l'm}_{lnl''m''} \right|^2$$
$$= \frac{B_l^2}{4\pi(2l'+1)} \sum_{n=-l}^{l} \sum_{m=-l'}^{l'} \left[\sum_{l_1''=0}^{\infty} \sqrt{2l_1''+1}\, C^{l'0}_{l0l_1''0} \sum_{l_2''=0}^{\infty} \sqrt{2l_2''+1}\, C^{l'0}_{l0l_2''0} \times \right.$$
$$\left. \sum_{m_2''=-l_2''}^{l_2''} \sum_{m_1''=-l_1''}^{l_1''} U_{l_1''m_1''}\, U^*_{l_2''m_2''}\, C^{l'm}_{lnl_1''m_1''}\, C^{l'm}_{lnl_2''m_2''} \right]$$
$$= \frac{B_l^2}{4\pi(2l'+1)} \sum_{l_1''=0}^{\infty} \sum_{l_2''=0}^{\infty} \sqrt{2l_1''+1}\sqrt{2l_2''+1}\, C^{l'0}_{l0l_1''0}\, C^{l'0}_{l0l_2''0} \times$$
$$\sum_{m_2''=-l_2''}^{l_2''} \sum_{m_1''=-l_1''}^{l_1''} U_{l_1''m_1''}\, U^*_{l_2''m_2''} \sum_{n=-l}^{l} \sum_{m=-l'}^{l'} C^{l'm}_{lnl_1''m_1''}\, C^{l'm}_{lnl_2''m_2''} \qquad \text{(B9)}$$

The last summation $\sum_{n=-l}^{l} \sum_{m=-l'}^{l'} C^{l'm}_{lnl_1''m_1''}\, C^{l'm}_{lnl_2''m_2''}$ simplifies to $(2l'+1)/(2l_1''+1)\delta_{l_1''l_2''}\delta_{m_1''m_2''}$ by Eq. (5) of § 8.7.2 of [41]. So, we have

$$A_{ll'} = \frac{B_l^2}{4\pi} \sum_{l''=|l-l'|}^{l+l'} \left(C^{l'0}_{l0l''0}\right)^2 \sum_{m''=-l''}^{l''} |U_{l''m''}|^2$$
$$= B_l^2 \frac{2l'+1}{4\pi} \sum_{l''=|l-l'|}^{l+l'} (2l''+1) \begin{pmatrix} l & l' & l'' \\ 0 & 0 & 0 \end{pmatrix}^2 \mathcal{U}_{l''}, \qquad \text{(B10)}$$

where $\mathcal{U}_{l''} \equiv \sum_{m''=-l''}^{l''} |U_{l''m''}|^2/(2l''+1)$. This matches the final expression of [27] (see Eq. [A31]).

3. The full sky limit with non-circular beam

The full sky limit to the final expression should reproduce the result obtained in [29]. We substitute $U_{lm} = \sqrt{4\pi}\delta_{l0}$ [$\Rightarrow\ U_{l''(m-n)} = \sqrt{4\pi}\delta_{l''0}\delta_{mn}$] in Eq (A12) and get

$$A_{ll'} = B_l^2 \frac{(2l'+1)}{4} \sum_{m=-\min(l,l')}^{\min(l,l')} \left| C^{l0}_{l000}\, C^{lm}_{lm00} \sum_{L=|l-l'|}^{l+l'} C^{L0}_{l-ml'm} \times \right.$$
$$\left. \sum_{N=-L}^{L} d^L_{0N}\left(\frac{\pi}{2}\right) \sum_{m'=-l'}^{l'} \beta_{l'm'}\, C^{Lm'}_{l0l'm'}\, d^L_{Nm'}\left(\frac{\pi}{2}\right) f(m';N) \right|^2 . \qquad \text{(B11)}$$

Using the relation $C^{c\gamma}_{a\alpha 00} = \delta_{ac}\delta\alpha\gamma$ (Eq. (2) in §8.5.1 of [41]) we may write $C^{l0}_{l000} = C^{lm}_{lm00} = 1$. Then rearranging terms, we may write

$$A_{ll'} = B_l^2 \frac{(2l'+1)}{4} \sum_{m=-\min(l,l')}^{\min(l,l')} \left| \sum_{m'=-l'}^{l'} \beta_{l'm'} \sum_{L=|l-l'|}^{l+l'} C^{L0}_{l-ml'm} C^{Lm'}_{l0l'm'} \times \sum_{N=-L}^{L} d^L_{0N}\left(\frac{\pi}{2}\right) d^L_{Nm'}\left(\frac{\pi}{2}\right) f(m';N) \right|^2 . \tag{B12}$$

Using the definition of $f(m';N)$ [Eq (E8)] and the expansion formula for Wigner-d [Eq (D15)] we may write

$$\sum_{N=-L}^{L} d^L_{0N}\left(\frac{\pi}{2}\right) d^L_{Nm'}\left(\frac{\pi}{2}\right) f(m';N) = \int_{-1}^{1} d\cos\theta\, d^L_{0m'}(\theta). \tag{B13}$$

Then, using the Clebsch-Gordon series [Eq. (E5)] we get

$$\sum_{L=|l-l'|}^{l+l'} C^{L0}_{l-ml'm}\, d^L_{0m'}(\theta)\, C^{Lm'}_{l0l'm'} = (-1)^m\, d^l_{m0}(\theta)\, d^{l'}_{mm'}(\theta). \tag{B14}$$

Finally, putting everything together, we get the expression for the bias matrix in the full sky limit with non-circular beam as

$$A_{ll'} = B_l^2 \frac{(2l'+1)}{4} \sum_{m=-\min(l,l')}^{\min(l,l')} \left| \sum_{m'=-l'}^{l'} \beta_{l'm'} \int_{-1}^{1} d\cos\theta\, d^l_{m0}(\theta)\, d^{l'}_{mm'}(\theta) \right|^2 , \tag{B15}$$

which matches Eq (38) of [29].

APPENDIX C: FAST COMPUTATION OF BIAS MATRIX FOR NON-CIRCULAR BEAM IN CMB ANALYSIS

The full expression for the bias matrix with no rotation ($\rho(q) = 0$):

$$A_{ll'} = B_l^2 \frac{2l'+1}{16\pi} \sum_{n=-l}^{l} \sum_{m=-l'}^{l'} \left| \sum_{l''=0}^{\infty} \sqrt{2l''+1}\, U_{l''(m-n)} \times \sum_{M''=-l''}^{l''} d^{l''}_{(m-n)M''}\left(\frac{\pi}{2}\right) d^{l''}_{M''0}\left(\frac{\pi}{2}\right) \sum_{M=-l}^{l} d^l_{nM}\left(\frac{\pi}{2}\right) d^l_{M0}\left(\frac{\pi}{2}\right) \times \sum_{M'=-l'}^{l'} d^{l'}_{mM'}\left(\frac{\pi}{2}\right) \sum_{m'=-l'}^{l'} \beta_{l'm'}\, d^{l'}_{M'm'}\left(\frac{\pi}{2}\right) f(m';M+M'+M'') \right|^2 . \tag{C1}$$

The following sequence of calculation is computationaly cost effective.. $V^{1,2,3}$ have been used as intermediate arrays. This prescription is only for the loops inside the modulus, so for each m, n pair all the three steps have to be performed.

- Step I:

$$V^1_{ll'}[N,m] = \sum_{M'=-l'}^{l'} d^{l'}_{mM'}\left(\frac{\pi}{2}\right) \sum_{m'=-l'}^{l'} \beta_{l'm'}\, d^{l'}_{M'm'}\left(\frac{\pi}{2}\right) f(m';M'+N), \tag{C2}$$

  N runs from $-(l+l''_{\max})$ to $+(l+l''_{\max})$.

- Step II

$$V^2_{ll'}[M'',n,m] = \sum_{M=-l}^{l} d^l_{nM}\left(\frac{\pi}{2}\right) d^l_{M0}\left(\frac{\pi}{2}\right) V^1_{ll'}[M+M'';m]. \tag{C3}$$

- Step III

$$V^3_{ll'}[m,n] = \sum_{l''=0}^{{l''}_{\max}} \sqrt{2l''+1}\, U_{l''(m-n)} \sum_{M''=-l''}^{l''} d^{l''}_{(m-n)M''}\left(\frac{\pi}{2}\right) d^{l''}_{M''0}\left(\frac{\pi}{2}\right) V^2_{ll'}[M'',n,m]. \tag{C4}$$

Required number of cycles to compute V^3 for each pair m,n (for $l_{\max} \gg {l''}_{\max}$):

$$\left[\{2(l+{l''}_{\max})+1\}(2l'+1)(2m'_{\max}+1) \;+\; (2{l''}_{\max}+1)(2l+1) + \sum_{l''=0}^{{l''}_{\max}}(2l''+1)\right] \tag{C5}$$

As mentioned earlier we are interested in the total number of computation cycles in the limit $l_{\max} \gg {l''}_{\max}$. Before proceeding further we note that $U_{l''m''} = U_{l''m-n}$ is limited to only m_{mask} modes for each l''. Here $m_{\text{mask}} > 0$. Then the condition for non zero $U_{lpp,m-n}$ becomes $|m-n| < m_{\text{mask}}$. This in turn implies that $m-n < m_{\text{mask}}$ when $m-n>0$, and $-m+n < m_{\text{mask}}$ when $m-n<0$. Then we see that for each n,m can run only from $n-m_{\text{mask}}$ to $n+m_{\text{mask}}$ for a total of $2m_{\text{mask}}+1$ values so that $U_{l''m-n}$ -s are non zero.

Thus considering two outer loops over m,n total computation cycles becomes

$$\begin{aligned}
&\sum_{l=2}^{l_{\max}}\sum_{l'=2}^{l_{\max}}(2l+1)(2m_{\text{mask}}+1)\;[\{2(l+l''_{\max})+1\}(2l'+1)(2m'_{\max}+1)+\\
&(2l''_{\max}+1)(2l+1)+\sum_{l''=0}^{l''_{\max}}(2l''+1)\Bigg]\\
=\;&(2m_{\text{mask}}+1)\sum_{l=2}^{l_{\max}}\sum_{l'=2}^{l_{\max}}(2l+1)\,[\{2(l+l''_{\max})+1\}(2l'+1)(2m'_{\max}+1)+\\
&(2l''_{\max}+1)(2l+1)+\sum_{l''=0}^{l''_{\max}}(2l''+1)\Bigg]\\
=\;&(2m_{\text{mask}}+1)\sum_{l=2}^{l_{\max}}\sum_{l'=2}^{l_{\max}}(2l+1)\,[2l''_{\max}(2l'+1)(2m'_{\max}+1)+\\
&(2l+1)(2l'+1)(2m'_{\max}+1)+(2l''_{\max}+1)(2l+1)+\sum_{l''=0}^{l''_{\max}}(2l''+1)\Bigg]
\end{aligned}$$

The computation cycles will be decided by the maximum power of the largest term in the above expression. Clearly the second term in the bracket will give the maximum contribution as it contains highest powers combined from l,l'. Hence the total number of cycles is

$$\begin{aligned}
(2m_{\text{mask}}+1)\sum_{l=2}^{l_{\max}}4l^2\sum_{l'=2}^{l_{\max}}(2l')(2m'_{\max}+1) \;&=\; (2m_{\text{mask}}+1)(2m'_{\max}+1)\;\times\\
8\left[\frac{l_{\max}(l_{\max}+1)(2l_{\max}+1)}{6}-1\right]&\left[\frac{l_{\max}(l_{\max}+1)}{2}-1\right]
\end{aligned} \tag{C6}$$

For $l_{\max} \gg 1$ the computation cost scales as $(4/3)(2m_{\text{mask}}+1)(2m'_{\max}+1)l^5_{\max}$.

APPENDIX D: EXPANSION OF WIGNER-D FUNCTION

1. Motivation

This derivation is motivated from Eq. (10) of §4.16 of [41]. However, the motivating equation is wrong, as it predicts $D^l_{mm'}(\phi,\theta,\rho) = 0$ if $m+m'odd$. We derive the correct formula by "reverse engineering". We start with the second

expression of the above mentioned equation [see below for steps]:

$$\begin{aligned}
&\sum_{M_1,M_2,M_3,M_4=-l}^{l}\Big[D^l_{mM_1}(\phi,0,0)\,D^l_{M_1M_2}\Big(0,\frac{\pi}{2},0\Big)\,D^l_{M_2M_3}(0,\theta,0)\,\times\\
&\quad D^l_{M_3M_4}\Big(0,\frac{\pi}{2},0\Big)\,D^l_{M_4m'}(0,0,\rho)\Big]\\
&=\ e^{-im\phi}\sum_{M_2,M_3=-l}^{l}\Big[D^l_{mM_2}\Big(0,\frac{\pi}{2},0\Big)\,D^l_{M_2M_3}(\theta,0,0)\,D^l_{M_3m'}\Big(0,\frac{\pi}{2},0\Big)\Big]\,e^{-im'\rho}\\
&=\ e^{-im\phi}\sum_{M_2=-l}^{l}\Big[D^l_{mM_2}\Big(0,\frac{\pi}{2},0\Big)\,D^l_{M_2m'}\Big(\theta,\frac{\pi}{2},0\Big)\Big]\,e^{-im'\rho}\\
&=\ e^{-im\phi}\,D^l_{mm'}\Big(\frac{\pi}{2},\pi-\theta,\frac{\pi}{2}\Big)\,e^{-im'\rho}\ =\ D^l_{mm'}\Big(\frac{\pi}{2}+\phi,\pi-\theta,\frac{\pi}{2}+\rho\Big)
\end{aligned}\tag{D1}$$

2. Steps

Step I

From Eq. (1) & (2) of §4.16, pg.112 of [41].

$$D^l_{mm'}(\phi,0,0)\ =\ e^{-im\phi}\,D^l_{mm'}(0,0,0)\tag{D2}$$
$$D^l_{mm'}(0,0,\rho)\ =\ D^l_{mm'}(0,0,0)\,e^{-im'\rho}\tag{D3}$$
$$D^l_{mm'}(0,0,0)\ =\ \delta_{mm'}.\tag{D4}$$

Step II

Another way is to combine the first two remaining D symbols using Eq. (1) of §4.16, pg.112 of [41] and then evaluate the following in Step III using the "Addition of Rotations" formula similar to the present method:

$$e^{-im\phi}\sum_{M_3=-l}^{l}\Big[D^l_{mM_3}\Big(0,\frac{\pi}{2},\theta\Big)\,D^l_{M_3m'}\Big(0,\frac{\pi}{2},0\Big)\Big]\,e^{-im'\rho}\tag{D5}$$

From the "Addition of Rotations" formula in Eq. (3) of §4.7, pg.87 of [41].

$$\sum_{M=-l}^{l}\big[D^l_{mM}(\phi,\theta_1,\gamma)\,D^l_{Mm'}(-\gamma,\theta_2,\rho)\big]\ =\ D^l_{mm'}(\phi,\theta_1+\theta_2,\rho).\tag{D6}$$

Step III

From Eq. (1) of §4.7, pg.87 of [41] we may write

$$\sum_{M=-l}^{l}\Big[D^l_{mM}(0,\frac{\pi}{2},0)\,D^l_{Mm'}(\theta,\frac{\pi}{2},0)\Big]\ =\ D^l_{mm'}(\alpha,\beta,\gamma)\tag{D7}$$

where α,β,γ are to be obtained using Eq. (66)-(70) of §1.4, pg.32 of [41]. Note that the arguments of the *first* D symbol have been denoted by $\alpha_2,\beta_2,\gamma_2$ respectively and *not* by $\alpha_1,\beta_1,\gamma_1$.
From Eq. (66) of §1.4, pg.32 of [41], since $0\le\alpha<2\pi, 0\le\beta\le\pi, 0\le\gamma<2\pi$

$$\cos\alpha\ =\ 0\ \Rightarrow\ \alpha\ =\ \frac{\pi}{2}\text{ or }\frac{3\pi}{2}\tag{D8}$$
$$\cos\beta\ =\ -\cos\theta\ \Rightarrow\ \beta\ =\ \pi-\theta\tag{D9}$$
$$\cos\gamma\ =\ 0\ \Rightarrow\ \gamma\ =\ \frac{\pi}{2}\text{ or }\frac{3\pi}{2}.\tag{D10}$$

From Eq. (67) of §1.4, pg.32 of [41]

$$\sin\alpha \;=\; \sin\gamma \;=\; \frac{\sin\theta}{\sin\theta} \;=\; 1. \tag{D11}$$

Combining the above equations we may write

$$\alpha \;=\; \frac{\pi}{2}; \quad \beta \;=\; \pi - \theta; \quad \gamma \;=\; \frac{\pi}{2}. \tag{D12}$$

3. Final expression

We can modify Eq. (D1) by changing $\phi \to \phi - \frac{\pi}{2}, \theta \to \pi - \theta, \rho \to \rho - \frac{\pi}{2}$ to reach the desired expansion:

$$\begin{aligned} D^l_{mm'}(\phi,\theta,\rho) \;&=\; e^{-im(\phi-\pi/2)} e^{-im'(\rho-\pi/2)} \;\times \\ &\sum_{M_2,M_3=-l}^{l} \left[D^l_{mM_2}\left(0,\frac{\pi}{2},0\right)\, D^l_{M_2M_3}(\pi-\theta,0,0)\, D^l_{M_3m'}\left(0,\frac{\pi}{2},0\right)\right]. \end{aligned} \tag{D13}$$

Then using the definitions of Wigner-d functions from Eq. (1) of §4.3, pg.76 and Eq. (1) of §4.16, pg.112 of [41], we get

$$D^l_{mm'}(\phi,\theta,\rho) \;=\; i^{m+m'} e^{-im\phi} \sum_{M=-l}^{l} \left[(-1)^M d^l_{mM}\left(\frac{\pi}{2}\right) e^{iM\theta} d^l_{Mm'}\left(\frac{\pi}{2}\right)\right] e^{-im'\rho}. \tag{D14}$$

This also means

$$d^l_{mm'}(\theta) \;=\; i^{m+m'} \sum_{M=-l}^{l} \left[(-1)^M d^l_{mM}\left(\frac{\pi}{2}\right) e^{iM\theta} d^l_{Mm'}\left(\frac{\pi}{2}\right)\right]. \tag{D15}$$

The coefficients $d^l_{mm'}(\pi/2)$ can be directly calculated using Eq. (5) of §4.16, pg.113 of [41]

$$\begin{aligned} d^l_{mm'}\left(\frac{\pi}{2}\right) \;&=\; (-1)^{m-m'} \frac{1}{2^l} \sqrt{\frac{(l+m)!(l-m)!}{(l+m')!(l-m')!}} \;\times \\ &\sum_{k=\max\{0,\,m'-m\}}^{\max\{l+m',\,l-m\}} (-1)^k \binom{l+m'}{k} \binom{l-m'}{k+m-m'}. \end{aligned} \tag{D16}$$

APPENDIX E: USEFUL FORMULAE

- Important relations [Eq. (1)s of §4.3, §4.17 & §5.4 and Eq. (2) of §4.4 of [41]]

$$D^l_{mm'}(\hat{\mathbf{q}},\rho) \;=\; e^{-im\phi}\, d^l_{mm'}(\theta)\, e^{-im'\rho} \tag{E1}$$

$$Y^*_{lm}(\hat{\mathbf{q}}) \;=\; \sqrt{\frac{2l+1}{4\pi}}\, D^l_{m0}(\hat{\mathbf{q}},\rho) \;=\; \sqrt{\frac{2l+1}{4\pi}}\, e^{-im\phi}\, d^l_{m0}(\theta) \tag{E2}$$

$$D^{l*}_{mm'}(\hat{\mathbf{q}},\rho) \;=\; (-1)^{m-m'}\, D^l_{-m-m'}(\hat{\mathbf{q}},\rho) \tag{E3}$$

$$Y^*_{lm}(\hat{\mathbf{q}}) \;=\; (-1)^m\, Y_{l-m}(\hat{\mathbf{q}}) \tag{E4}$$

  Note that, unlike [29], the argument of the Wigner-d function is θ (standard definition) *not* $\cos\theta$.

- The Clebsch-Gordon series:
  Expansion of the product of two Wigner-D functions [Eq (1) of §4.6 of [41]]:

$$\begin{aligned} &D^{l_1}_{m_1n_1}(\hat{\mathbf{q}},\rho)\, D^{l_2}_{m_2n_2}(\hat{\mathbf{q}},\rho) \;= \\ &\sum_{l=|l_1-l_2|}^{l_1+l_2} C^{l(m_1+m_2)}_{l_1m_1l_2m_2}\, D^l_{(m_1+m_2)(n_1+n_2)}(\hat{\mathbf{q}},\rho)\, C^{l(n_1+n_2)}_{l_1n_1l_2n_2}, \end{aligned} \tag{E5}$$

where $C^{lm}_{l_1m_1l_2m_2}$ are the Clebsch-Gordon coefficients.
The special case of spherical harmonics [Eq. (9) of §5.6 of [41]]:

$$Y_{l_1m_1}(\hat{\mathbf{q}})\,Y_{l_2m_2}(\hat{\mathbf{q}}) \;= \sum_{l=|l_1-l_2|}^{l_1+l_2} \sqrt{\frac{(2l_1+1)(2l_2+1)}{4\pi(2l+1)}}\, C^{l0}_{l_10l_20}\, C^{l(m_1+m_2)}_{l_1m_1l_2m_2}\, Y_{l(m_1+m_2)}(\hat{\mathbf{q}}). \tag{E6}$$

In modifying the above equations (from [41]) we have used the fact that the Clebsch-Gordon coefficients $C^{lm}_{l_1m_1l_2m_2}$ vanish if $m \neq m_1 + m_2$.

- The integral $\int_0^\pi d\theta\, \sin\theta\, e^{iN\theta}$ evaluates to

$$\int_0^\pi d\theta \left[\frac{e^{i(N+1)\theta} - e^{i(N-1)\theta}}{2i}\right] = \begin{cases} \pm i\pi/2 & \text{if } N = \pm 1 \\ \left[\frac{1-e^{i(N+1)\pi}}{2(N+1)} - \frac{1-e^{i(N-1)\pi}}{2(N-1)}\right] & = \begin{cases} 0 & \text{if } N = odd\ (\neq \pm 1) \\ \frac{2}{1-N^2} & \text{if } N = 0, even. \end{cases} \end{cases} \tag{E7}$$

The above can be used to define an useful quantity

$$\begin{aligned} f(m';N) \;&:=\; \Re\left[i^{m'}\,(-1)^N \int_0^\pi \sin\theta d\theta\, e^{iN\theta}\right] \\ &= \begin{cases} (-1)^{(m'\pm 1)/2}\,\pi/2 & \text{if } m' = odd \text{ and } N = \pm 1 \\ (-1)^{m'/2}\,2/(1-N^2) & \text{if both } m', N = 0 \text{ or } even \\ 0 & \text{otherwise.} \end{cases} \end{aligned} \tag{E8}$$

---

[1] W. Hu and S. Dodelson, Ann. Rev. of Astron. and Astrophys. **40**, 171 (2002).
[2] J. R. Bond, *Theory and Observations of the Cosmic Background Radiation*, in *Cosmology and Large Scale Structure*, Les Houches Session LX, August 1993, ed. R. Schaeffer, (Elsevier Science Press, 1996).
[3] G. Efstathiou, Mon. Not. Roy. Astron. Soc. **349**, 603 (2004).
[4] K. M. Gorski, Astrophys. J. Lett., **430**, L85, (1994).
[5] K. M. Gorski, et.al., Astrophys. J. Lett., **430**, L89, (1994).
[6] K. M. Gorski, et.al., Astrophys. J. Lett., **464**, L11, (1996).
[7] K. M. Gorski, in *the Proceedings of the XXXIst Recontres de Moriond,'Microwave Background Anisotropies'*, (1997); astro-ph/9701191.
[8] M. Tegmark, Phys. Rev. **D55**, 5895, (1997).
[9] J. R. Bond, A. H. Jaffe and L. Knox, Phys. Rev. **D 57**, 2117, (1998).
[10] J. Borrill, Phys. Rev. **D 59**, 27302 (1999); J. Borrill in *Proceedings of the 5th European SGI/Cray MPP Workshop*, (1999); astro-ph/9911389.
[11] J. R. Bond, R. G. Crittenden, A. H. Jaffe, L. Knox, Comput.Sci.Eng. **1**, 21 (1999).
[12] S. P. Oh, D. N. Spergel and G. Hinshaw, Astrophys. J. **510**, 551, (1999).
[13] O. Dore, L.Knox and A. Peel, Phys. Rev. **D 64**, 3001, (2001).
[14] U. L. Pen, Mon. Not. Roy. Astron. Soc., **346**, 619, (2001).
[15] A. D. Challinor et al., Mon. Not. Roy. Astron. Soc. **331**, 994, (2002); F. van Leeuwen et al., Mon. Not. Roy. Astron. Soc. **331**, 975, (2002).
[16] B. D. Wandelt and F. Hansen, Phys. Rev. **D 67**, 23001, (2003).
[17] B. D. Wandelt, *Talk from PhyStat2003, Stanford, Ca, USA*; astro-ph/0401623.
[18] J. Jewell, S. Levin, C.H. Anderson, 2004, Astrophys. J. **609**, 1, (2004), [astro-ph/0209560].
[19] L. Knox, N. Christensen & C. Skordis, Astrophys. J. **563**, L95, (2001).
[20] J. T. Yu and P. J. E. Peebles, Astrophys. J. **158**, 103, (1969).
[21] P. J. E. Peebles, Astrophys. J. **185**, 431, (1974).
[22] B. Wandelt, E. Hivon and K. M. Gorski, Phys. Rev. **D 64**, 083003 (2003).
[23] I. Szapudi, S. Prunet, D. Pogosyan, A. Szalay, J. R. Bond, Astrophys. J. **548**, L115, (2001).
[24] I. Szapudi, S. Prunet, S. Colombi, Astrophys. J. **561**, L11, (2001).
[25] C. L. Bennett et.al., Astrophys. J. Suppl., **148**, 1, (2003).
[26] G. Hinshaw et.al., Astrophys. J. Suppl.,**148**, 135, (2003).
[27] E. Hivon, K. M. Gorski, C. B. Netterfield, B. P. Crill, S. Prunet and F. Hansen, Astrophys. J. **567**, 2, (2002).

[28] M. L. Brown, P. G. Castro, A. N. Taylor, Mon.Not.Roy.Astron.Soc. **360**, 1262, (2005).
[29] S. Mitra, A. S. Sengupta and T. Souradeep, Phys. Rev. D **70**, 103002 (2004).
[30] T. Souradeep and B. Ratra, Astrophys. J. **560** 28 (2001)
[31] P. Fosalba, O. Dore and F. R. Bouchet, Phys. Rev. **D 65**, 063003 (2002).
[32] G. Hinshaw *et al.*, *preprint* [arXiv: astro-ph/0603451].
[33] D. J. Mortlock, A. D. Challinor and M. P. Hobson, Mon. Not. Roy. Astron. Soc. **330**, 405 (2002).
[34] K. Coble et al., Astrophys. J. **584**, 585, (2003); P. Mukherjee et al., Astrophys. J. **592**, 692, (2003).
[35] T. Risbo, Journal of Geodesy, **70**, 383 (1996).
[36] G. Efstathiou, Mon. Not. Roy. Astron. Soc., **370**, 343 (2006).
[37] R. Saha, P. Jain and T Souradeep, Astrophys.J. **645**, L89 (2006); astro-ph/0508383.
[38] A. Hajian and T. Souradeep, Astrophys. J. **597**, L5 (2003).
[39] J. M. Kovac et al., Nature **420**, 772, (2002).
[40] A. Kogut, et.al., Astrophys.J.Suppl., **148**, 161 (2003).
[41] D. A. Varshalovich, A. N. Moskalev and V. K. Khersonskii (VMK), *Quantum theory of angular momentum*, World Scientific, (1988).
[42] D. Spergel *et al.*, *preprint* [arXiv: astro-ph/0603449].
[43] A. Hajian & T. Souradeep & N. Cornish, Astrophys. J. Lett. **618**, L63 (2004); astro-ph/0406354.
[44] A. Hajian & T. Souradeep, Phys.Rev. **D 74**, 123521 (2006); astro-ph/0607153.
[45] S. Basak, A. Hajian & T. Souradeep, Phys. Rev. **D 74**, 021301(R) (2006).
[46] E. M. Leitch, J. M. Kovac, N. W. Halverson, J. E. Carlstrom, C. Pryke and M. W. E. Smith Astrophys. J. **624**, 10, (2005).
[47] F. Piacentini *et al.*, Astrophys. J. **647**, 833 (2006); astro-ph/0507507; C. J. MacTavish *et al.*, Astrophys. J. **647**, 799 (2006); astro-ph/0507503.
[48] L. Page et al., *preprint*, [arXiv:astro-ph/0603450].
[49] For concreteness , we consider the example of Kp2 mask used in the WMAP analysis Here, for simplicity we do not consider the excised point sources. As this mask has also 0.6 degree radius cut around 208 locations of the point sources we first fill them up, except few, very near the galactic plane.